



# Investigation on the nature of active species in the $\text{CeCl}_3$ -doped sodium alanate system

Xiulin Fan, Xuezhong Xiao, Lixin Chen\*, Shouquan Li, Qidong Wang

Department of Materials Science and Engineering, Zhejiang University, 38 Zheda Road, Hangzhou 310027, People's Republic of China

## ARTICLE INFO

### Article history:

Received 21 July 2010

Received in revised form

28 September 2010

Accepted 13 October 2010

Available online 23 October 2010

### Key words:

Sodium alanate

Hydrogen storage

Active species

$\text{CeAl}_4$

$\text{CeCl}_3$

## ABSTRACT

$\text{CeCl}_3$ -doped  $\text{NaAlH}_4$  was directly synthesized in hydrogenation process using  $\text{NaH}/\text{Al}$  with 2 mol%  $\text{CeCl}_3$  under ball-milling. X-ray diffraction was utilized to unveil the nature of cerium during  $\text{NaAlH}_4$  synthesis process and succedent cycling. It is found that,  $\text{CeCl}_3$  is reduced in the ball-milling process and following cycles, causing the formation of  $\text{NaCl}$  and  $\text{Al}-\text{Ce}$  alloy with a structure of  $\text{CeAl}_4$ . The catalytic enhancement arising upon doping the ball-milled  $\text{CeAl}_4$  alloy is quite similar to that achieved in the  $\text{CeCl}_3$ -doped sodium alanate. Because the  $\text{CeAl}_4$  dopant does not consume the effective hydrogen storage component, the  $\text{CeAl}_4$ -doped  $\text{NaAlH}_4$  exhibits more hydrogen storage capacity. Moreover,  $\text{CeCl}_3$ -doped  $\text{NaAlH}_4$  and  $\text{CeAl}_4$ -doped  $\text{NaAlH}_4$  exhibit similar apparent activation energies estimated from Kissinger's method, suggesting the reactions are all determined by the same rate-limiting step. These results clearly demonstrate that the in situ formed  $\text{CeAl}_4$  acts as active species to catalyze the reversible dehydrogenation/rehydrogenation of  $\text{NaAlH}_4$ .

© 2010 Elsevier B.V. All rights reserved.

## 1. Introduction

Since the discovery of the catalytic effect of Ti halide precursors [1],  $\text{NaAlH}_4$  has become a promising candidate for the solid-state storage of hydrogen. Extensive research has been focused on the sodium alanate, especially for the exploration of the dopants [2–6]. Heretofore, the most effective dopants are still halides, in particular  $\text{TiCl}_3$  and  $\text{CeCl}_3$  [5,7]. With the aid of these halides,  $\text{NaAlH}_4$  can be hydrogenated and dehydrogenated under technically applicable conditions. Therefore, understanding of the catalytic mechanism in the metal-doped  $\text{NaAlH}_4$  system has been a subject of great interest. During the past decade, several species have been proposed as the active species in the Ti-doped sodium alanate [4,7–13], yet the empirical results show that these species are all significantly inferior to that arising upon doping the hydrides with halide dopant precursors [3,8,14].

For the  $\text{CeCl}_3$ -doped  $\text{NaAlH}_4$ , the mechanism of the enhancement of the kinetics is not revealed, neither is the nature of active cerium species. According to the amount of hydrogen evolved during ball-milling, Bogdanović et al. [5] suggested that the metals may exist in zero-valent or hydridic forms in their active states. Recently, Léon et al. [15] found that the no formation of a bimetallic entity consisting of Ce and Al which is the case in Ti doped sample can be detected. Instead of that, the authors report oxidation state of

Ce(III) remains constant during preparation and cycling. In contrast, our recent work [16] shows that Ce–Al phase with a structure of  $\text{CeAl}_4$  will be formed during the dehydrogenation of the first cycle. To gain further understanding of the catalytic effect of the  $\text{CeCl}_3$  dopant, we therefore decided to investigate this problem in more detail to picture the nature of active cerium species. For this purpose, a systematic structure/property investigation has provided convincing the evidence of the nature of active cerium species in the Ce-doped  $\text{NaAlH}_4$ .

## 2. Experimental

Directly synthesis of metal-doped  $\text{NaAlH}_4$  from  $\text{NaH}/\text{Al}$  and additives by ball-milling has been utilized as a novel method to prepare the hydrogen storage materials [17]. This novel method not only further improves the kinetics of the rehydrogenation process of the material, but also provides a perspective to probe and testify the nature of active metal species.

### 2.1. Sample preparation

All samples were prepared and handled in an argon-filled glovebox with the oxygen and water concentrations below 1 ppm.  $\text{NaH}$  (Aldrich, 95%, <74  $\mu\text{m}$ ),  $\text{Al}$  powder (Aldrich, 99.9%, <74  $\mu\text{m}$ ) and  $\text{CeCl}_3$  (Alfa Aesar, anhydrous, 99.5%) were used as received. The catalyst of the  $\text{CeAl}_4$  was prepared by induction melting stoichiometric mixtures of pure Ce (99.9%) and Al (99.9%) metals in argon atmosphere. The as-prepared  $\text{CeAl}_4$  was smashed and then mechanically milled for 10 h under argon atmosphere by the Planetary mill at 300 rpm to prepare powder precursors.

The powder mixture of  $\text{NaH}$ ,  $\text{Al}$ , and  $\text{CeCl}_3$  or  $\text{CeAl}_4$  with a molar ratio of 1:1:0.02 was milled in the Planetary ball mill (QM-3SP4J, Nanjing) at 350 rpm under a hydrogen pressure of 3 MPa. Around 2 g of mixture was prepared each time. The vial is made of stainless steel and the volume is 120 ml. The ball is made of stainless steel with a diameter of 1 cm. The ball-to-powder weight ratio was around 60:1. The G-

\* Corresponding author. Tel.: +86 571 8795 1152; fax: +86 571 8795 1152.  
E-mail address: [lxchen@zju.edu.cn](mailto:lxchen@zju.edu.cn) (L. Chen).

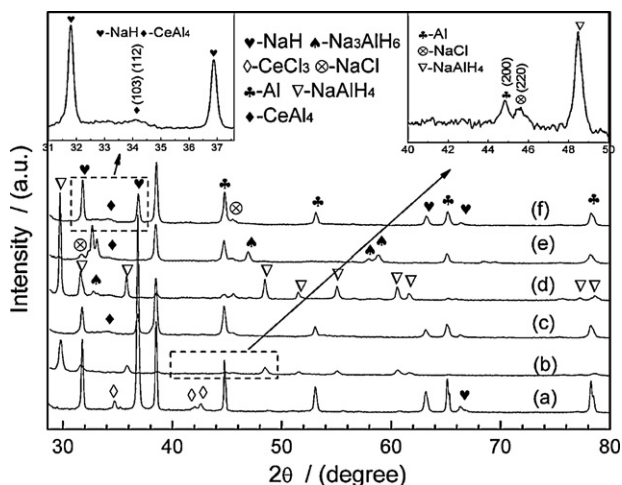


**Fig. 1.** XRD patterns collected in the synthesis and the following dehydrogenation–rehydrogenation cycles of  $\text{CeCl}_3$ -doped  $\text{NaAlH}_4$ : (a) starting materials before ball-milling; (b) milled for 80 h; (c) after dehydrogenation of the first cycle at  $170^\circ\text{C}$ ; (d) after rehydrogenation of ninth cycle; (e) after dehydrogenation of tenth cycle at  $120^\circ\text{C}$ ; (f) after dehydrogenation of tenth cycle at  $170^\circ\text{C}$ .

forces generated in the process of milling was about 8.57 g. In a parallel investigation for comparison, the powder mixture of NaH and Al without the dopant was prepared in the same way.

## 2.2. Characterization

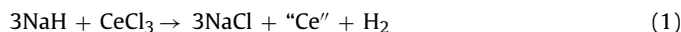
Dehydrogenation and rehydrogenation cycling of the prepared samples were carried out on a calibrated Sievert's type apparatus. The volume of sample holder is about 2.5 ml. A sample of about 0.7 g was tested. The sample holder had a thermocouple located in the center of the sample to monitor temperature in the reaction zone. For hydrogenation, the sample was first heated to the temperature of  $120^\circ\text{C}$ , and then pressurized with 11 MPa  $\text{H}_2$ . After hydrogenation, the pressure decreased to 10.00–10.40 MPa due to hydrogen uptake by the sample. For dehydrogenation, the measurements proceeded against a constant pressure of 1 atm. The apparatus was heated at first to  $120^\circ\text{C}$  and then to  $170^\circ\text{C}$  (first and second dehydrogenation step). It should be noted that the wt% of hydrogen is calculated on the basis of the total weight of the samples including the weight of dopants.

X-ray diffraction (XRD) experiments of the samples were performed on the ARL X'TRA diffractometer (Thermo Electron Corp.) with  $\text{Cu-K}\alpha$  radiation. The data were collected in the range between  $28^\circ$  and  $80^\circ$  with a step width of  $0.02^\circ$  at a rate of  $2.5^\circ/\text{min}$ . The DSC measurements were performed on a Netzsch STA 449F3 instrument. A sample of about 5 mg was tested using 0.1 MPa of argon as the purge gas with a rate of 40 ml/min. Special caution had been taken to prevent the  $\text{H}_2\text{O}/\text{O}_2$  contamination during the measurements.

## 3. Results and discussion

### 3.1. X-ray diffraction analysis

Fig. 1. shows the XRD patterns collected in the synthesis and the following dehydrogenation–rehydrogenation cycles of  $\text{CeCl}_3$ -doped  $\text{NaAlH}_4$ . It shows that after a milling time of 80 h, NaH and Al are almost completely transformed to  $\text{NaAlH}_4$ . Meanwhile, NaCl phase is detected at  $2\theta = 45.7^\circ$  according to JCPDS 05-0628 while  $\text{CeCl}_3$  disappears (Fig. 1b). However, no Ce-containing phases can be observed, which probably are disordered/amorphous after ball milling. This phenomenon is quite similar to the  $\text{TiCl}_3$ -doped  $\text{NaAlH}_4$  [10,18]. Based on these facts, we can conclude that during the synthesis the dopant of  $\text{CeCl}_3$  will react with NaH, resulting in the formation of NaCl and “Ce” entity. The reaction can be assumed to be:



After the synthesis, the dehydrogenation–rehydrogenation cycling of the  $\text{CeCl}_3$ -doped  $\text{NaAlH}_4$  was carried out. After the first dehydrogenation,  $\text{CeAl}_4$  is observed (Fig. 1c), which remains almost

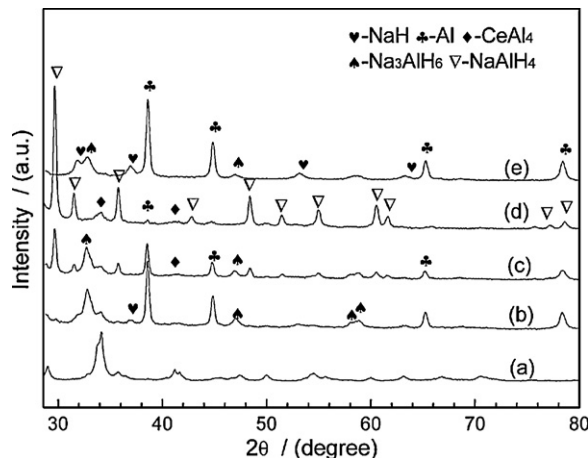


**Fig. 2.** XRD patterns of dopant  $\text{CeAl}_4$  ball-milled for 10 h (a) and comparison of XRD patterns obtained during the ball milling of 2 mol%  $\text{CeAl}_4$ -doped and undoped NaH/Al: 2 mol%  $\text{CeAl}_4$ -doped NaH/Al milled for 40 h (b); milled for 80 h (c); milled for 100 h (d); undoped NaH/Al milled for 100 h (e).

unchanged in the process of following cycles. The broad peak at  $2\theta = 34^\circ$  can be assigned to the overlap of (1 1 2) and (1 0 3) diffraction of the  $\text{CeAl}_4$  phase according to JCPDS 65-2678. The formation of  $\text{CeAl}_4$  can be postulated to be:



In the cycling,  $\text{CeAl}_4$  is identified as the sole newly formed Ce-containing species in the XRD examination. The result clearly suggests a possible correlation between the formed  $\text{CeAl}_4$  and catalytic enhancement achieved in the  $\text{CeCl}_3$ -doped  $\text{NaAlH}_4$ .

To check this possibility,  $\text{CeAl}_4$  was directly utilized as the dopant precursor and mechanically milled with NaH/Al mixture under a hydrogen pressure of 3 MPa. As the catalyst, the catalytic enhancement will exhibit effectively only if the parent hydrides and the catalyst can integrate effectually. The direct synthesis method provides us a simple way, which may suffice for this possibility. During ball milling, the instant temperature and the higher pressure conditions created by collision among the balls and between the vial wall and the balls may favor the integration of the dopant and the parent hydrides. The selection XRD patterns of the synthesis of  $\text{CeAl}_4$ -doped  $\text{NaAlH}_4$  are shown in Fig. 2. As can be seen from the figure, the mixture of NaH/Al with 2 mol%  $\text{CeAl}_4$  exhibits similar behaviors during ball milling: NaH reacts with Al and  $\text{H}_2$  resulting in the formation of  $\text{Na}_3\text{AlH}_6$ , then the formed  $\text{Na}_3\text{AlH}_6$  and Al transforms to  $\text{NaAlH}_4$  under relatively high  $\text{H}_2$  pressure. After a milling time of about 100 h, the mixture almost totally transforms to  $\text{NaAlH}_4$  (Fig. 2d). In a comparative investigation, we failed in our attempt to synthesize  $\text{NaAlH}_4$  just from the mixture of NaH/Al without any dopants under identical milling conditions. After 100 h milling time, only part of  $\text{Na}_3\text{AlH}_6$  came into being (Fig. 2e). Therefore, it can be concluded that the doped  $\text{CeAl}_4$  plays a critical role in the formation of  $\text{NaAlH}_4$ .

### 3.2. Hydrogen storage properties examination

If the in situ formed  $\text{CeAl}_4$  surely is the active species in the  $\text{CeCl}_3$ -doped  $\text{NaAlH}_4$ , effectively doping the  $\text{CeAl}_4$  to the hydrides should result in the similar kinetics. Comparative hydrogenation curves for  $\text{CeCl}_3$ - and  $\text{CeAl}_4$ -doped  $\text{NaAlH}_4$  are shown in Fig. 3. As can be seen, the hydrogenation for the  $\text{CeCl}_3$ -doped  $\text{NaAlH}_4$  exhibits a good cycle stability, which can be reloaded in 25 min. No obvious deterioration can be found in the tested cycles. This is in good agreement with previous investigations [5,17]. As for the  $\text{CeAl}_4$ -doped  $\text{NaAlH}_4$ , its kinetics underwent a little degradation

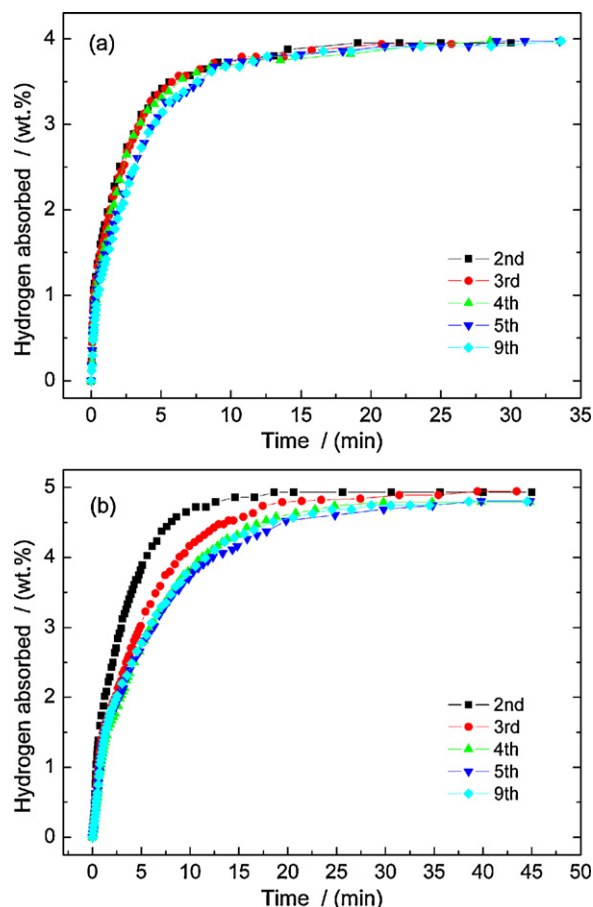


**Fig. 3.** Comparison on the hydrogenation profiles between the directly synthesized  $\text{CeCl}_3$ -doped  $\text{NaAlH}_4$  (a), and  $\text{CeAl}_4$ -doped  $\text{NaAlH}_4$  (b).

during the first 3 cycles and then stabilized. For catalyzed reactions, the practical catalytic effectiveness relies not only on the intrinsic activity of the catalyst, but also on the distribution state of the catalyst particles. In the case of the hydrides doped with  $\text{CeCl}_3$ , it is believed that the  $\text{CeCl}_3$  can react with  $\text{NaH}$  and  $\text{Al}$  forming a much high dispersion of  $\text{CeAl}_4$  in the hydride matrix. However, by directly doping the  $\text{CeAl}_4$  into the hydrides, the particle size and the dispersion will all be inferior to that of the in situ formed  $\text{CeAl}_4$ , which may caused these differences in the catalytic performance.

Because the dopant of  $\text{CeAl}_4$  does not consume the effective hydrogen storage constitute,  $\text{CeAl}_4$ -doped  $\text{NaAlH}_4$  exhibits a higher hydrogen capacity compared with that of  $\text{CeCl}_3$ -doped  $\text{NaAlH}_4$ . As can be seen from Fig. 3(b), the capacity level of 4.8 wt% at the end of the cycling test can be attained after 40 min, while for  $\text{CeCl}_3$ -doped  $\text{NaAlH}_4$ , only about 4.0 wt% can be achieved.

To investigate the catalytic effect on dehydrogenation, the thermal decomposition behaviors of  $\text{NaAlH}_4$  doped with 2 mol%  $\text{CeCl}_3$  and  $\text{CeAl}_4$  were characterized by the DSC curves shown in Fig. 4a. The two distinct endothermic peaks of the curves correspond to the two hydrogen desorption steps. Compared to the undoped  $\text{NaAlH}_4$ , which cannot release hydrogen till the temperature reaches  $185^\circ\text{C}$  for  $\text{NaAlH}_4$  and  $230^\circ\text{C}$  for  $\text{Na}_3\text{AlH}_6$ , the dopants of  $\text{CeCl}_3$  and  $\text{CeAl}_4$  can lower the desorption temperature drastically. The first step displays a considerable desorption rate already at about  $110^\circ\text{C}$ , with its peak at  $139.9^\circ\text{C}$  for  $\text{CeCl}_3$ -doped  $\text{NaAlH}_4$  and  $140.8^\circ\text{C}$  for  $\text{CeAl}_4$ -doped  $\text{NaAlH}_4$ , respectively. The second step will start to decompose before the first step completely finished, and exhibits the peak at  $164.1^\circ\text{C}$  for  $\text{CeCl}_3$ -doped  $\text{NaAlH}_4$  and  $171.2^\circ\text{C}$  for  $\text{CeAl}_4$ -doped  $\text{NaAlH}_4$ .

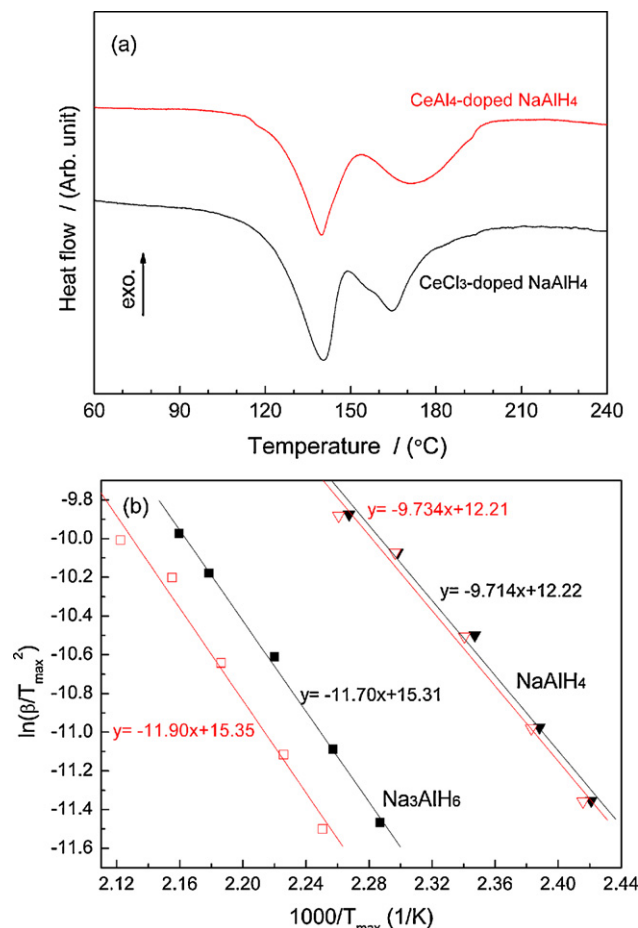


**Fig. 4.** (a) DSC traces at a heating rate of  $2^\circ\text{C}/\text{min}$  for  $\text{CeCl}_3$ - and  $\text{CeAl}_4$ -doped  $\text{NaAlH}_4$  after the second hydrogenation. (b) Kissinger plots for the first and the second decomposition of  $\text{CeCl}_3$  (solid symbols, dark line) and  $\text{CeAl}_4$ -doped (open symbols, red line)  $\text{NaAlH}_4$ . (For interpretation of the references to color in this figure legend, the reader is referred to the web version of the article.)

The activation energy of  $\text{NaAlH}_4$  and  $\text{Na}_3\text{AlH}_6$  for hydrogen desorption can be calculated using a Kissinger analysis that is based on the shifts in  $T_{\text{max}}$  with heating rate ( $\beta$ ) of 2, 3, 5, 8, and  $10^\circ\text{C}/\text{min}^{-1}$  [19]. For that,  $\ln(\beta/T_{\text{max}}^2)$  was plotted versus  $1/T_{\text{max}}$  (see Fig. 4b). The slope of the curve represents  $-E_a/R$  in which  $R$  is the molar gas constant. The values of  $E_a$  for the first and the second dehydrogenation are summarized in Table 1. As a comparison, the calculated  $E_a$  of the undoped  $\text{NaAlH}_4$  are also presented. It can be seen that after doping the additives, the activation energy all lowered significantly.

Interestingly, almost the same activation energies were obtained for the  $\text{CeCl}_3$ - and  $\text{CeAl}_4$ -doped  $\text{NaAlH}_4$  of either the first step or the second step. An explanation for the coincidence of  $E_a$  can be deduced from the findings reported by Sandrock et al. [20] and Kircher and Fichtner [21]. They demonstrated that increasing the dopant concentration will result a faster decomposition, however, the  $E_a$  turns out to be identical for all the doped samples. As to our experiment, in situ formed  $\text{CeAl}_4$  may exhibit smaller

**Table 1**  
Experimental activation energy  $E_a$  calculated using a Kissinger analysis.

Dopant	Activation energy $E_a$ (kJ/mol)	
	$\text{NaAlH}_4$	$\text{Na}_3\text{AlH}_6$
2 mol% $\text{CeCl}_3$	80.76	97.27
2 mol% $\text{CeAl}_4$	80.93	98.94
Nothing	114.2	156.8

particle size and disperse more homogeneously, however, it just influences the hydriding and dehydriding rate. Although the exact mechanism of catalysis is as yet unknown, we can assume that during the process of dehydrogenation the  $\text{CeAl}_4$ , either in situ formed or the directly doped, will catalyze the transformation of  $\text{NaAlH}_4$  and may form the same transition state, which eventually results in the same activation energy.

#### 4. Conclusions

By XRD investigations carried out on the samples of  $\text{CeCl}_3$ -doped  $\text{NaAlH}_4$  in the course of synthesis and following cycles, it can be concluded that  $\text{CeCl}_3$  reacts with hydrides in the ball milling, causing the formation of  $\text{NaCl}$ , and probably widely dispersed  $\text{Ce}$  entity or the  $\text{Ce-Al}$  cluster with poor crystallinity that cannot be detected by XRD examination. After the first dehydrogenation, as the sole newly detected  $\text{Ce}$ -containing species,  $\text{Al-Ce}$  alloy with a structure of  $\text{CeAl}_4$  comes into being, and remains almost unchanged in the following hydrogenation and dehydrogenation cycles. The comparative study shows that, doping the as-prepared  $\text{CeAl}_4$  to the hydrides using direct synthesis method can result in comparable hydrogen absorption and desorption kinetics. The addition of  $\text{CeCl}_3$  and  $\text{CeAl}_4$  can significantly lower the thermal activation energy for both decomposition steps to the similar values. These results clearly demonstrate that the in situ formed  $\text{CeAl}_4$  acts as active species to catalyze the reversible dehydrogenation and rehydrogenation of  $\text{NaAlH}_4$ .

#### Acknowledgements

The financial supports for this research from the National Basic Research Program of China (2007CB209701), the National Natural

Science Foundation of China (50871099, 50631020), the program for New Century Excellent Talents in Universities (NCET-07-0741) and the University Doctoral Foundation of the Ministry of Education (20090101110050) are gratefully acknowledged.

#### References

- [1] B. Bogdanović, M. Schwickardi, *J. Alloys Compd.* 253 (1997) 1–9.
- [2] B. Bogdanović, M. Felderhoff, S. Kaskel, A. Pommerin, K. Schlichte, F. Shüth, *Adv. Mater.* 15 (2003) 1012–1015.
- [3] M. Resan, M.D. Hampton, J.K. Lomness, D.K. Slattery, *Int. J. Hydrogen Energy* 30 (2005) 1417–1421.
- [4] E.H. Majzoub, K.J. Gross, *J. Alloys Compd.* 356 (2003) 363–367.
- [5] B. Bogdanović, M. Felderhoff, A. Pommerin, F. Shüth, N. Spielkamp, *Adv. Mater.* 18 (2006) 1198–1201.
- [6] T. Sun, B. Zhou, H. Wang, M. Zhu, *Int. J. Hydrogen Energy* 33 (2008) 2260–2267.
- [7] A. Léon, G. Yalovega, A. Soldatov, M. Fichtner, *J. Phys. Chem. C* 112 (2008) 12545–12549.
- [8] P. Wang, X.D. Kang, H.M. Cheng, *J. Phys. Chem. B* 109 (2005) 20131–20136.
- [9] C.P. Baldé, H.A. Stil, A.M.J. van der Eerden, K.P. de Jong, J.H. Bitter, *J. Phys. Chem. C* 111 (2007) 2797–2802.
- [10] H.W. Brinks, B.C. Hauback, S.S. Srinivasan, C.M. Jensen, *J. Phys. Chem. B* 109 (2005) 15780–15785.
- [11] J. Liu, Q. Ge, *Chem. Commun.* (2006) 1822–1824.
- [12] F. Fang, J. Zhang, J. Zhu, G.R. Chen, D.L. Sun, B. He, Z. Wei, S.Q. Wei, *J. Phys. Chem. C* 111 (2007) 3476–3479.
- [13] J. Íñiguez, T. Yildirim, *Appl. Phys. Lett.* 86 (2005) 103109.
- [14] X.D. Kang, P. Wang, X.P. Song, X.D. Yao, G.Q. Lu, H.M. Cheng, *J. Alloys Compd.* 424 (2006) 365–369.
- [15] A. Léon, J. Rothe, K. Chłopek, O. Zabara, M. Fichtner, *Phys. Chem. Chem. Phys.* 11 (2009) 8829–8834.
- [16] X.L. Fan, X.Z. Xiao, L.X. Chen, K.R. Yu, Z. Wu, S.Q. Li, Q.D. Wang, *Chem. Commun.* (2009) 6857–6859.
- [17] B. Bogdanović, M. Felderhoff, A. Pommerin, F. Shüth, N. Spielkamp, A. Stark, *J. Alloys Compd.* 471 (2009) 383–386.
- [18] C. Weidenthaler, A. Pommerin, M. Felderhoff, B. Bogdanović, F. Shüth, *Phys. Chem. Chem. Phys.* 5 (2003) 5149–5153.
- [19] H.E. Kissinger, *Anal. Chem.* 29 (1957) 1702–1706.
- [20] G. Sandrock, K. Gross, G. Thomas, *J. Alloys Compd.* 339 (2002) 299–308.
- [21] O. Kircher, M. Fichtner, *J. Alloys Compd.* 404 (2005) 339–342.